ISSN 0022-0930, Journal of Evolutionary Biochemistry and Physiology, 2023, Vol. 59, No. 2, pp. 369–381. © Pleiades Publishing, Ltd., 2023.
Russian Text © The Author(s), 2023, published in Zhurnal Evolyutsionnoi Biokhimii i Fiziologii, 2023, Vol. 59, No. 2, pp. 131–142.

EXPERIMENTAL PAPERS

Passive Membrane Properties and Spike Characteristics in a Pair of Identified Electrically Coupled *Lymnaea stagnalis* Neurons under Long-Term Experimental Hyperglycemia

A. V. Sidorov[a,*] and V. N. Shadenko[a,b]

[a] *Belarusian State University, Minsk, Belarus*

[b] *Republican Research and Practice Center for Mental Health, Minsk, Belarus*
**e-mail: sidorov@bsu.by*

Received December 6, 2022; revised January 15, 2023; accepted January 17, 2023

Abstract—Microelectrode technique was used to study the responses of the electrically coupled giant peptidergic VD1 and RPaD2 neurons within the isolated CNS of the pond snail *Lymnaea stagnalis* to prolonged (≥ 2 h) exposure to high D-glucose concentrations (10 mM). It has been established that passive membrane properties of the RPaD2, compared to VD1, undergo significant changes under experimental hyperglycemia—a decrease in membrane resistance (R_m) accompanied by an increase in membrane capacitance (C_m) and time constant (τ_m). Despite the invariance of VD1 and RPaD2 firing rates, the VD1 membrane depolarized, while the RPaD2 membrane potential did not vary significantly. Modifications in temporal, but not amplitude, characteristics of VD1 and RPaD2 action potentials were similar and resulted in a prolongation of their main phases (rising, falling, undershoot). It is assumed that the "unification" of membrane electrical properties in *L. stagnalis* CNS neurosecretory neurons (VD1/RPaD2) under hyperglycemia plays an adaptive role, aimed at overcoming the possible desynchronization of their spike activity due to electrical decoupling initiated by a high glucose content in the interstitial space.

DOI: 10.1134/S0022093023020060

Keywords: glucose, electrical synapse, nervous system, homeostasis, mollusks, invertebrates

INTRODUCTION

Pacemaker neurons are key elements of the oscillator-based central pattern generators (CPGs) in the nervous system of both vertebrates and invertebrates [1, 2]. Their invariable feature is the capacity to constantly generate action potentials, even in the absence of extraneous synaptic inputs. Typically, this feature owes to the special passive properties of their membranes, providing repetitive spike trains [3]. In combination with electrical synapses, which link CPGs with many surrounding neurons, this allows synchronizing the electrical activity of large neuronal ensembles within a particular brain region [4, 5].

It is traditionally believed that, despite their autonomy, CPGs are subject to modulatory influences of external factors, including those mediated by various signaling molecules [6]. Glucose ranks a special position among their multitude, being a universal nutrient used by nerve cells both to satisfy their metabolic needs and as a signaling molecule, the sensitivity to which characterizes not only the neurons involved in eating behavior

control, but also the brain as a whole [7, 8]. In other words, glucose can act as a volume transmission factor, the responsiveness to which is not confined to a handful of specialized cells.

The frequency component of the action potentials (spikes) generated by nerve cells, which represent an excitation wave periodically arising on the neuronal membrane, is of leading importance in the reaction of nerve cells. Spike characteristics (temporal and amplitude) can differ considerably both in neurons of different types, and in the same cell, depending, for example, on the frequency of its firing [9]. Such a so-called action potential plasticity is important for the functioning of neural networks, as it predetermines the depolarization (degree and duration) of nerve endings, which in turn directly mediates the amount of neurotransmitter released and the efficiency of synaptic transmission between nerve center cells [10]. However, the extent of our knowledge on the plasticity of spikes depending on the functional specialization of neurons and/or their neurotransmitter specificity is rather limited, primarily due to insufficient brain mapping in higher vertebrates.

The central nervous system (CNS) of the mollusk *Lymnaea stagnalis* contains a pair of electrically coupled nerve cells (VD1/RPaD2) belonging to the peptidergic multifunctional neurons, which are part of at least the cardioregulatory neural network [11, 12]. The sensitivity of these, likewise other peptidergic neurons in the *L. stagnalis* CNS, to the effect of glucose during rapid (for minutes) changes in its content in the external milieu has been previously shown [13]. Meanwhile, fluctuations in blood (hemolymph) glucose levels in a given mollusk reach significant ranges, from the basal level of 0.2–0.3 mM to 5 mM and probably more, if it concerns various functional states related with the activation of food consumption [14]. Each of these states is characterized by its own repertoire of behavioral reactions, which makes assuming that changes occur at the neuronal level as well, caused by the prolonged (for hours) action of elevated glucose levels. To assess the presence or absence of the possibility to modify electrical spike characteristics of the identified neurons in the *L. stagnalis* CNS under hyperglycemic conditions, as well as the membrane mechanisms of their sensitivity/resistance to hyperglycemia, was the aim of this work.

MATERIALS AND METHODS

Animals. The work was carried out on a freshwater pond snail *Lymnaea stagnalis.* Mollusks were collected in the summer and fall periods in shallow reservoirs of the Vabich and Drut river basins (Mogilev Region, Belarus). In the laboratory, they were kept in aquaria with settled tap water ($\geq$ 1 L per individual) at a temperature of 20 ± 1°C. The animals were fed ad libitum on young lettuce leaves. Control and experimental groups were completed with size-matched mollusks having a shell height from 3.5 to 4.5 cm and weighing from 2 to 4 g.

Electrophysiology. The animals were anesthetized (0.2 M $MgCl_2$, 5 min); the circumesophageal nerve ring was removed, and its constituent ganglia were treated with pronase solution (Protease E, type XIV, Sigma, USA; 1 mg/mL, 5 min). Electrical activity recording started at least 30 min after washing the preparation with Ringer's solution for *L. stagnalis* (in mM): NaCl, 44; KCl, 1.7; $CaCl_2$, 4; $MgCl_2$, 1.5; HEPES (N-2-hydroxyethylpiperazine-N-2-ethane sulfonic acid), 10, pH 7.5 ± 0.1. D-glucose solutions (analytic grade, Analysis X, Belarus) were prepared on its basis. To assess the prolonged effects of hyperglycemia, CNS preparations were incubated in 10 mM glucose solution for at least 2 h. The preparations kept in pure Ringer's solution for the same time served as controls.

A pair of electrically coupled neurons (VD1/RPaD2) residing in the visceral and right parietal ganglia were identified by their location within the ganglia (Fig. 1a), size, color, as well as the indices and pattern of spontaneous electrical activity [15].

Electrical activity of the neurons was recorded via glass microelectrodes filled with 2.5 M KCl solution (resistance, 10–15 MΩ). A chlorinated silver wire served as an indifferent electrode. Intracellular signals were amplified, and de- or hyperpolarizing current pulses were fed using an MS-01M microelectrode amplifier (Lintech, Belarus). Neuronal electrical signals were predigitized and recorded on a hard disk. Current moni-

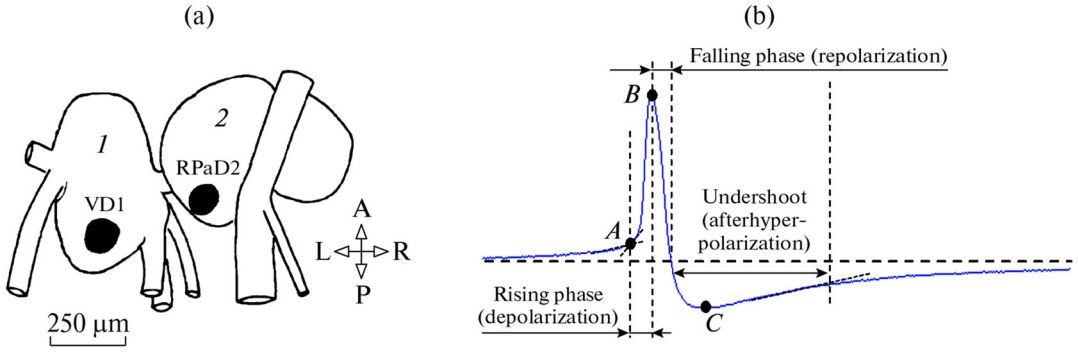

Fig. 1. Location of VD1/RPaD2 neurons in the *Lymnaea stagnalis* CNS (a), temporal and amplitude spike (action potential) characteristics (b). For (a): *1*—visceral ganglion, *2*—right parietal ganglion; A—anterior, P—posterior, L—left, R—right. For (b): Spike phases: rising, falling, undershoot. *A*—Threshold, *B*—positive peak value, *C*—negative peak value.

toring, recording and subsequent signal computation were carried out using the InputWin electronic oscilloscope software [16].

The firing rate was determined for 4 consecutive 30-s segments of the 2-min neuronogram (quantization step, 5 ms). Action potential (spike) parameters, including the duration and amplitude of its phases (Fig. 1b), were assessed for 4 randomly selected spikes by 30-s neuronogram segments performed with a quantization step size of 0.5 ms. The threshold amplitude was counted off from the resting potential level until a regenerative increase in sodium conductance (point A), the spike amplitude—up to a positive (point B) and undershoot amplitude—down to a negative (point C) peak value of a spike. The segment from the point A to that of intersection between the recording curve and the membrane potential level [its total (A) and average (A/t) areas, calculated with allowance for the phase duration, are expressed in conventional machine units, m.u.] was taken as a positive spike phase, while the undershoot segment was taken as a negative phase.

The membrane time constant (τ_m) was determined by the change in the membrane potential induced by a –0.5 nA current pulse as the time when it reaches $1/e$ of the maximally observed; the membrane capacitance (C_m) was calculated by the formula $\tau_m = R_m \times C_m$, where R_m is the membrane resistance determined from the cell input resistance at a –0.5 nA current pulse after deduction of microelectrode resistance and with no concern for the axoplasm and extracellular medium resistance. To plot a membrane current-voltage curve (I–V curve), 3-s current pulses were fed in series within the range from –2 to +2 nA (with a 0.5 nA step), simultaneously recording membrane potential values of the cells being studied. The obtained data were presented graphically.

Statistics. Normality of distribution for each series of experimental data was pre-assessed using the Shapiro–Wilk W-test. If normal distribution of the parameters to be compared was confirmed, the parametric statistical methods, such as the Student's t-test for independent pairs and repeated measures ANOVA, were used. If normal distribution was not confirmed for all data groups without exception, the nonparametric Mann–Whitney U-test (z) for pairwise comparison of independent samples was applied. Data were presented as $M \pm SEM$ (for normal distribution) or median with upper and lower quartiles (for nonparametric distributions). The number of observations (n) was given for each data array individually. The data were processed using the Statistica 6.0 software. The differences were considered statistically significant at $p < 0.05$.

RESULTS

Passive membrane properties. Under control conditions, the VD1 membrane resistance (R_m) was 2.5-fold lower ($t = 3.99$; $p < 0.01$), while the capacitance (C_m) was 5.2-fold higher ($t = 2.59$; $p = 0.02$) compared to those of RPaD2. Differences in the membrane time constant (τ_m) were statistically non-significant ($t = 1.39$; $p = 0.19$).

Table 1. Passive membrane properties of VD1 and RPaD2 neurons

Parameters	VD1		RPaD2	
	Control ($n = 9$)	Glucose, 10 mM ($n = 7$)	Control ($n = 5$)	Glucose, 10 mM ($n = 5$)
Resistance (R_m), MΩ	25.1 ± 5.3	21.0 ± 3.6 $t = 0.63$; $p = 0.54$	63.0 ± 8.5	30.0 ± 8.0* $t = 2.83$; $p = 0.02$
Capacitance (C_m), nF	14.1 ± 3.2	26.4 ± 5.5 $t = 2.04$; $p = 0.06$	2.7 ± 0.4	14.8 ± 2.1* $t = 5.71$; $p < 0.001$
Time constant (τ_m), ms	261 ± 54	468 ± 83* $t = 2.17$; $p < 0.05$	127.0 ± 11.3	388 ± 64* $t = 3.53$; $p < 0.01$

Data presented as $M \pm SEM$. For the experimental groups, the Student's t-test significance level (p) vs. control are given for each parameters and neuron. *—statistically significant changes.

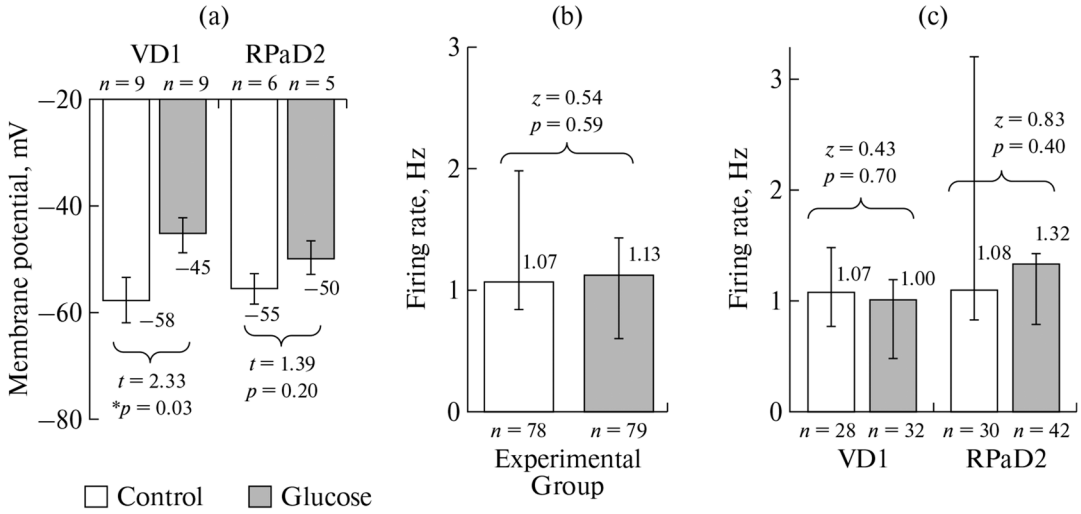

Fig. 2. Membrane potential (a) and firing rate (b, c) in the pair of electrically coupled *L. stagnalis* neurons VD1/RPaD2 in control (Control) and under experimental hyperglycemia (Glucose). (a) Resting potential, (b) summarily for both neurons, (c) separately for each neuron. The numbers above the columns (M for (a), or median for (b, c)) and error bars (SEM for (a), or lower and upper quartiles for (b, c)) indicate the values of the above parameters; n—the number of neurons studied (a), or the number of 30-s neuronogram segments analyzed (for (b, c)). For each comparison group, t (Student's t-test, for (a)) or z (Mann–Whitney U-test, for (b, c)), as well as significance level (p), values are indicated. *—Statistically significant changes.

Under hyperglycemia, there was a significant 1.79-fold increase in τ_m for VD1, while other membrane electrical characteristics of this neuron remained invariable. By contrast, a 2.1-fold decrease in R_m was observed for RPaD2, accompanied by a multiple (5.5-fold) increase in C_m against the background of a moderate (1.2-fold) decrease in τ_m compared to the control. Under these conditions, no differences were detected between R_m ($t = 1.18$; $p = 0.26$), C_m ($t = 1.28$; $p = 0.23$), and τ_m ($t = 0.31$; $p = 0.76$) of VD1 and RPaD2 neurons (Table 1).

Differences in the resting potential between VD1 and RPaD2, were non-significant in both control ($t = 0.40$; $p = 0.70$) and hyperglycemic conditions ($t = 0.91$; $p = 0.38$). At the same time, an increase in the interstitial glucose content led to depolarization of VD1 (by 10–15 mV, i.e., 1.3-fold vs. control), but did not change the level of RPaD2 membrane potential (Fig. 2a). The rate of firing between VD1 and RPaD2 was apparently invariable in both control ($z = 1.30$; $p = 0.19$) and hyperglycemic ($z = 1.73$; $p = 0.08$) conditions. The development of hyperglycemia did not

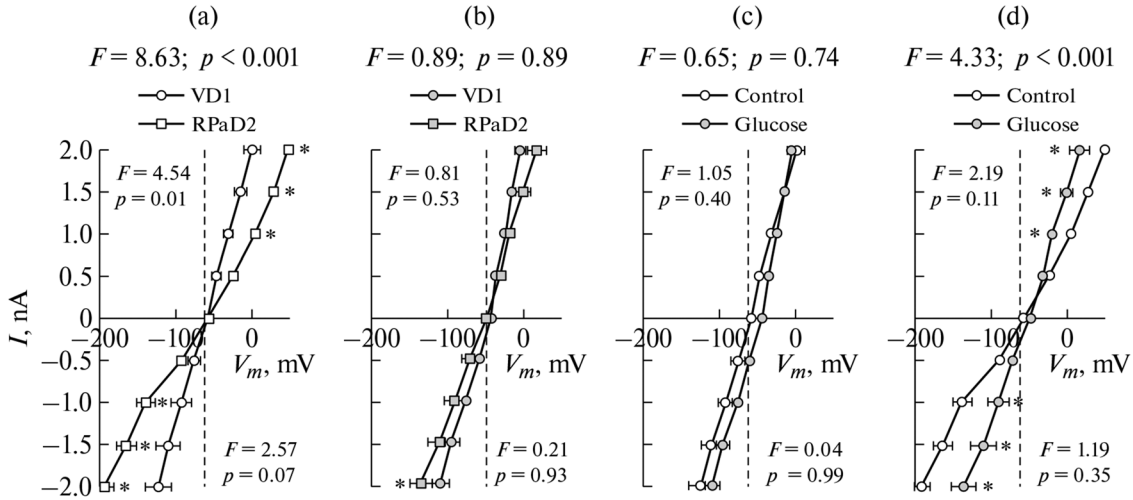

Fig. 3. Current-voltage curve (I-V curve) for the membrane of electrically coupled VD1 and RPaD2 neurons. (a) Control, (b) hyperglycemia, (c) VD1 neuron, (d) RPaD2 neuron. *F*—*F*-test; *p*—significance level for repeated measures ANOVA, including separately for positive (upper left) and negative (lower right) currents. The vertical dashed line is given for better obviousness of changes in the I–V curve. *—Statistically significant changes (pairwise comparison).

change the spike characteristics of this pair of electrically coupled cells (Fig. 2b), including those of each individual neuron (Fig. 2c).

Under control conditions, the I-V curve for the RPaD2 membrane was shifted rightward in the area of positive (outward) currents and leftward in the area of negative (inward) currents relative to that of VD1 (Fig. 3a). Under hyperglycemic conditions, there was no statistically significant differences in the I–V curve between VD1 and RPaD2 neurons (Fig. 3b). An analysis carried out for each individual neuron in the pair revealed a statistical invariance of the I-V curve for VD1 (Fig. 3c) and its shift—leftward for outward currents and rightward for inward currents—for RPaD2 (Fig. 3d) under hyperglycemic vs. control conditions.

Spike characteristics. Under control conditions, there were marked differences, mainly in the temporal spike characteristics, between VD1 and RPaD2 neurons (Fig. 4). These differences were concerned with an increase in the duration of depolarization (rising) and repolarization (falling) phases, respectively, by 1.36 ($z = 2.03$; $p = 0.04$) and 2.44 ($z = 4.83$; $p < 0.001$) times and a decrease in the undershoot duration by 1.65 ($z = 3.79$; $p < 0.001$) times for RPaD2 vs. VD1 neurons. The values of the spike amplitude ($z = 0.94$; $p = 0.35$) and its threshold ($z = 1.64$; $p = 0.10$), in contrast to a 2.22-fold decrease in the undershoot values ($z = 4.02$; $p < 0.001$), did not differ significantly. Under hyperglycemic conditions, both temporal [duration of the rising ($z = 1.81$; $p = 0.07$), falling ($z = 1.62$; $p = 0.11$) and undershoot ($z = 1.60$; $p = 0.11$) phases] and amplitude [threshold ($z = 0.71$; $p = 0.48$), spike ($z = 1.40$; $p = 0.16$) and undershoot ($z = 1.24$; $p = 0.21$) amplitudes] spike characteristics in VD1 and RPaD2 neurons were statistically indistinguishable.

A more detailed analysis revealed in the VD1a neuron spike a statistically significant 1.43-fold increase in the rising phase duration (Fig. 4a) and by far more considerable (2.0-fold), albeit statistically non-significant, increase in the falling phase duration (Fig. 4b) under experimental hyperglycemia compared to control. A significant increase was also observed in the duration of the undershoot phase, by a factor of 1.33 for the experimental (hyperglycemic) conditions compared to control (Fig. 4c). As for the amplitude of the spike phases, statistically significant changes were found in none of the parameters studied—action potential, threshold of its generation, and undershoot (Figs. 4d–4f)—under experimental hyperglycemia compared to control. In the RPaD2 neuron, the duration of the rising (Fig. 4a) and undershoot (Fig. 4c) phases increased 1.21- and 2.02-fold, respectively, with a downward tendency for the falling phase duration (Fig. 4b). At

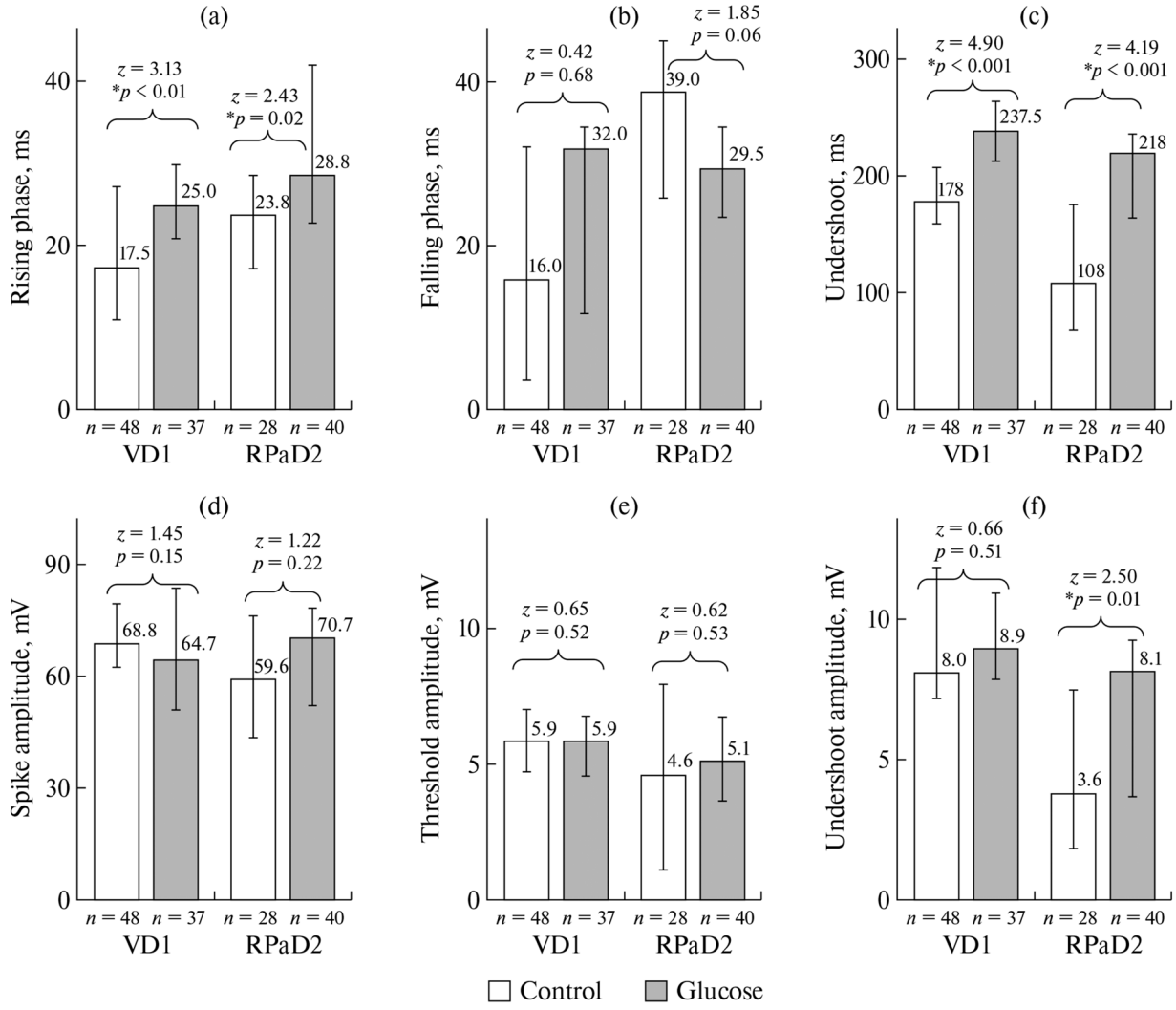

Fig. 4. Spike temporal and amplitude characteristics in VD1 and RPaD2 neurons under control (Control) and hyperglycemic (Glucose) conditions. (a) Rising (depolarization) phase duration; (b) falling (repolarization) phase duration; (c) undershoot (afterhyperpolarization) phase duration; (d) spike amplitude; (e) threshold amplitude; (f) undershoot amplitude. The numbers above the columns (median) and error bars (lower and upper quartiles), as well as the number of spikes analyzed (*n*), describe the characteristics studied here. For each comparison group, *z* (Mann-Whitney *U*-test) and significance level (*p*) values are indicated. *—Statistically significant changes.

the same time, statistically significant differences were only recorded for the undershoot amplitude (2.25-fold increase, Fig. 4f), with the values of the spike (Fig. 4d) and threshold (Fig. 3e) amplitudes being invariant.

Changes in the spike shape, recorded during hyperglycemia in VD1 and RPaD2 neurons, concerned both type I spikes, “narrow”, with approximately the same duration of rising and falling phases, characteristic of low or moderate (on average, 0 5 Hz and less) firing rates (Figs. 5a, 6a), and type 2 spikes, “wide”, with a small plateau during the falling phase, which makes it longer compared to the rising phase, recorded mainly at high (1.0 Hz and above) firing rates (Figs. 5b, 6b). Also notable was an increase in the rate of slow membrane depolarization under hyperglycemia (Figs. 5, 6, areas *A*), as well as in the undershoot intensity (Figs. 5, 6, area *B*), mainly for type 2 spikes (in VD1).

The absence of statistical significance for changes in the falling phase duration (Fig. 4b), despite a considerable, sometimes 2-fold, difference in median values, is due to the use of both

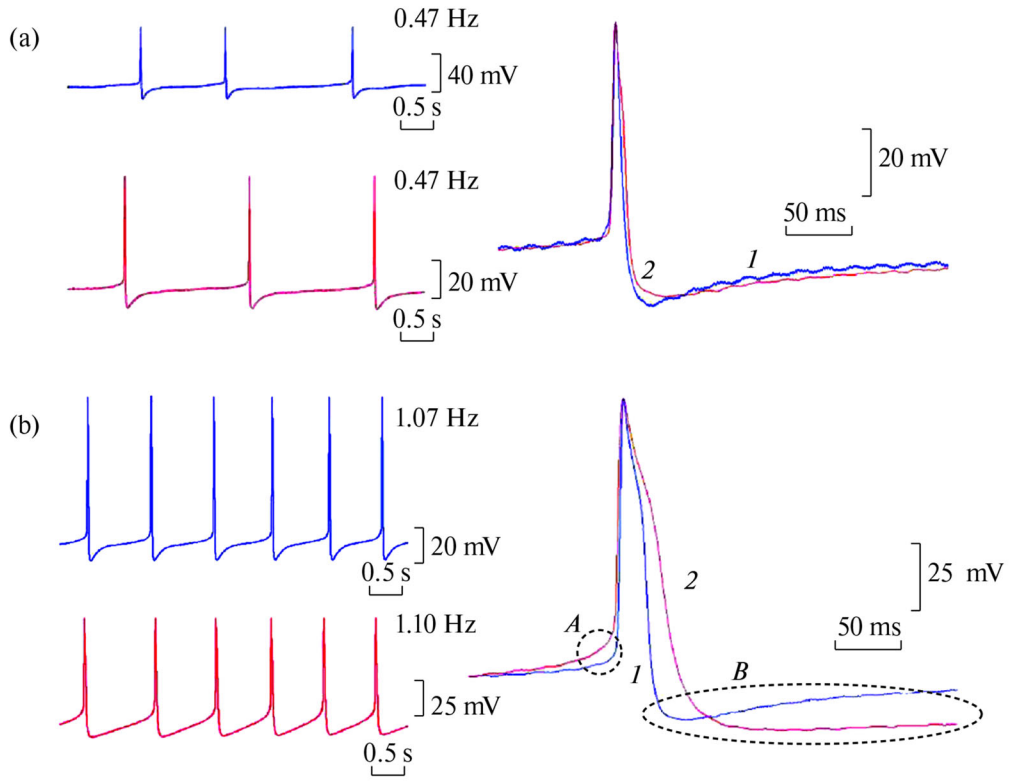

Fig. 5. Spontaneous electrical activity of the VD1 neuron and the shape of its different spike types in control and experimental hyperglycemia. (a) Type 1 spikes, (b) type 2 spikes. For (a–b): left—5-s record fragment: upper trace (blue)—control, bottom trace (red)—hyperglycemia (glucose, 10 mM); right—overlay of individual spikes [blue (*1*)—control, red (*2*)—glucose, 10 mM] in this fragment with the overlapping of their positive peak and resting potential values, accompanied by a vertical alignment of spike amplitudes relative to the height of the Figure via a graphics editor, which illustrates the dynamics of spike temporal characteristics. Records of VD1 spontaneous electrical activity under control and hyperglycemic conditions were obtained from different CNS preparations. For record fragments (left), the frequency values (Hz) are shown; calibration is indicated for each record separately. Record fragments, reflecting changes in slow depolarization and undershoot, are accentuated by dashed lines (areas *A* and *B*, respectively).

type I and type II spikes for the calculation of spike parameters, whose proportion (occurrence) in the preparations of control vs. experimental groups are different (approximately 1 : 3 and 1 : 1, respectively). As a consequence, the magnitude of statistical straggling, especially in the control group, levels off the significance of the observed differences. We deemed incorrect to normalize these data (i.e., actually to discard these or those values) in terms of the design of experiments.

Such integral spike characteristics as the areas (total and average) of its phases were significantly different from each other when comparing data for VD1 and RPaD2 neurons (Fig. 7). Under control conditions, a 1.77-fold increase ($z = 2.12$; $p = 0.03$) and a 2.75-fold decrease ($z = 2.36$; $p = 0.02$) in the total area of the positive and negative spike phases, respectively, was observed in RPaD2 vs. VD1 neurons. At the same time, the average area of spike phases in RPaD2 was 1.10 ($z = 4.76$; $p < 0.001$) and 2.11 ($z = 5.09$; $p < 0.001$) times smaller compared to that in VD1 for the positive and negative phases, respectively. Under hyperglycemia, these differences and their directionality between VD1 and RPaD2 generally persisted, except for the values of the total positive phase area ($z = 0.02$; $p = 0.98$). For RPaD2 vs. VD1 spikes, there was a 1.94-fold decrease in the total area of the positive phase ($z = 2.97$; $p < 0.01$), as well as a 1.27-fold ($z = 2.80$; $p < 0.01$) and 1.75-fold ($z = 3.88$; $p < 0.001$) decrease in the average areas of the positive and negative phases, respectively.

Under hyperglycemic vs. control conditions, the total spike area in the VD1 neuron increased 1.32- and 2.49-fold for the positive and negative

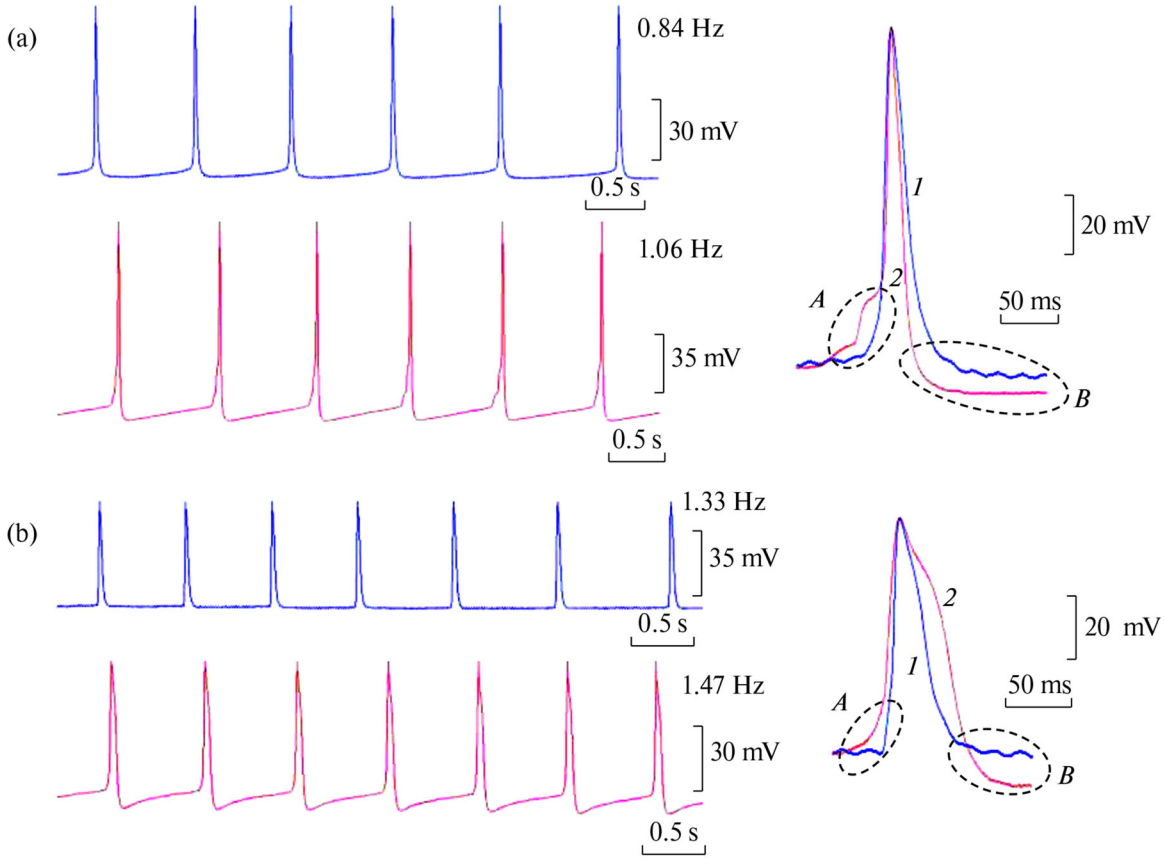

Fig. 6. Spontaneous electrical activity of the RPaD2 neuron and the shape of its different spike types in control and experimental hyperglycemia. (a) Type 1 spikes, (b) type 2 spikes. Other notes as in Fig. 5.

phases, respectively (Fig. 7a), while the average phase area increased 1.26- (positive phase) and 1.29-fold (negative phase) (Fig. 7b). In the RPaD2 neuron, the values of the total and average area of the positive spike phase were invariant, while the same values for its negative phase increased 3.53- and 1.55-fold with the increasing of the interstitial glucose content.

DISCUSSION

The cytoplasms of electrically coupled VD1/RPaD2 neurons are actually interlinked via innexons (low-resistance contacts, gap junctions, providing a direct communication of these cells) [17] based on transmembrane, aqueous pore-forming, channel proteins—innexins [18, 19]. As a consequence, the thus formed electrical circuit includes three sequentially connected elements, each with its individual electrical characteristics (resistance and capacitance): presynaptic cell (an input integrator), gap junctions, and postsynaptic cell. Since in the configuration, we used in our experiments, there was neither mechanical separation of the neurons nor voltage clamp on their membrane, it is more correct to speak about the electrical properties of the chain of electrically connected neurons, which are, nevertheless, determined mainly by the characteristics of the presynaptic neuron.

In these terms, the values that we determined for the membrane resistance should have been lower and for the capacitance higher than those for isolated neurons—an increase in the total membrane area allows holding a large amount of charge (capacity is higher) and also increases the number of pathways for currents flowing through the membrane (resistance is lower). Indeed, Benjamin et al. [17] pointed out that R_m was 50 MΩ for VD1 and 68 MΩ for RPaD2, and it was emphasized separately that this parameter was quite variable, fluctuating in the range of 14–

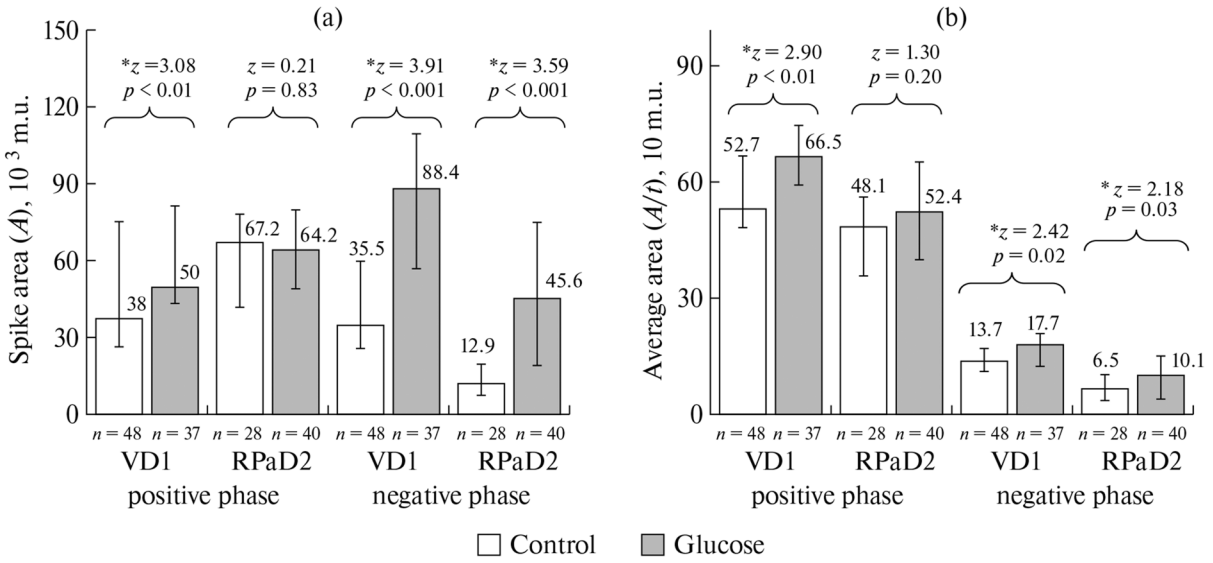

Fig. 7. Spike integral parameters in VD1 and RPaD2 neurons in control (Control) and under experimental hyperglycemia (Glucose). (a) Total area (*A*) of the spike phase (positive/negative), (b) average area (*A*/*t*) of the spike phase (positive/negative). The numbers above the columns (median) and error bars (lower, upper quartiles)—parameter values; *n*—the number of spikes analyzed. For each comparison group, *z* (Mann–Whitney *U*-test) and *p* (significance level) values are indicated. *—Significant changes; m.u.—machine units.

80 MΩ. The τ_m value, determined in the same work, showed no statistically significant differences for VD1 and RPaD2, being about 300 ms, which is generally typical for molluskan neurons [20]. On the other hand, there are reports of significantly higher R_m values for VD1 and RPaD2, reaching ~300 and ~350 MΩ, respectively, while the τ_m value was reduced, respectively, to ~120 and ~200 ms [21], yielding the calculated values for C_m of the order of 0.4 and 0.6 nF. Such fluctuations of the "normative" values have been assumed to be related with the seasonal plasticity of pond snail neurons [22]. However, the manufacturing and fixation peculiarities of the isolated CNS preparation should not also be ruled out as they can considerably affect the integrity of neuron–neuron communication (the gap junction area falls on the contact area of their axons [17], while the neurons themselves, as noted above, are located in different, albeit neighboring, ganglia).

Under hyperglycemic conditions, there was a decrease in membrane resistance (R_m), especially noticeable in the RPaD2 neuron (see Table data and I–V curve shift in Fig. 3d), which may indicate an increase in transmembrane fluxes of various ions, primarily Na^+, Ca^{2+} and K^+, as it was described a number of vertebrate [23] and invertebrate nerve cells [24]. In addition, there was an "alignment" of R_m for VD1 and RPaD2: I–V curves for these cells almost completely coincided under hyperglycemia. As a consequence, the VD1/RPaD2 coupling ratio (*CR*) changes (decreases), at least during signal transmission in one of the possible directions (from VD1 to RPaD2), as it depends on R_m of a conditionally postsynaptic cell [25]: $CR = R_m / (R_m + r_c)$, where r_c—coupling resistance. This is confirmed by the presence of electrotonic excitatory postsynaptic potentials recorded on the RPaD2 membrane in some isolated CNS preparations (Fig. 8) and corresponding to the development of a full-fledged spike in VD1. A similar situation is observed exactly when r_c increases, i.e., when the VD1/RPaD2 coupling ratio decreases (see [17], Fig. 11).

Various intracellular metabolites (H^+, Ca^{2+}, reactive oxygen species, etc.) are known to exert a pronounced effect on gap junction conductivity [26, 27]. Their increased interstitial levels are usually associated with cell membrane disintegration, i.e. cell death resulting in VD1/RPaD2 coupling ratio reduction, which permits thereby to isolate such a brain region from the surrounding intact cells [28]. The possibility of glucose interaction

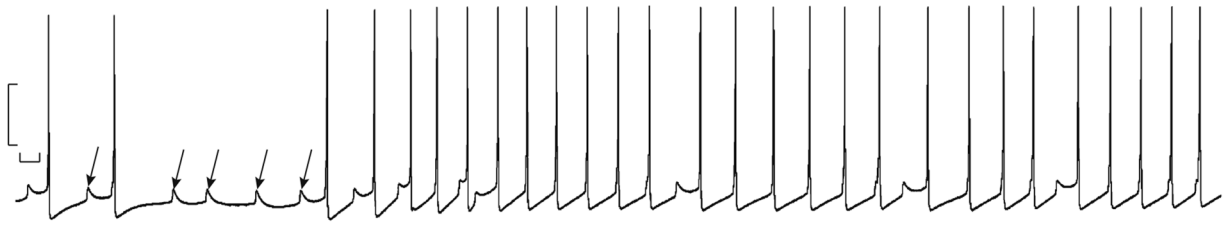

Fig. 8. Spontaneous electrical activity of the *Lymnaea stagnalis* RPaD2 neuron under experimental hyperglycemia. Local potentials that do not turn into action potentials are marked with arrows. Calibration: time—0.5 s, amplitude—35 mV.

with membrane proteins and various components in the perimembranous space, leading to a change in the membrane's charge-holding capacity, is indicated by the increase in membrane capacitance and, hence, in membrane time constant, as observed in the present work. A similar mechanism is suggested for the effect of some anesthetics, which markedly alter the excitability of *L. stagnalis* nerve cells [21].

The "alignment" of VD1 and RPaD2 electrical characteristics under hyperglycemic conditions can be exemplified even better by changes in the spike shape. These changes manifest themselves in spike "stretching", i.e. the increasing of the duration of spike phases with the constancy of amplitude characteristics: relatively "narrow" spikes in the VD1 neuron widen and become indistinguishable from those in RPaD2. Such a reaction can be due to increased duration for certain plasma membrane ion channels to stay in the open (or closed) state with a relative invariance of their number, as indicated by the time course (hours) of the observed effect: mass renewal of plasma membrane channel proteins requires by far more time [29].

Rising phase elongation was obviously associated with the increase in Na^+ conductance, probably due to the intensification of Na^+/glucose cotransporter activity, as it was reported for a number of peptidergic neurosecretory cells in *L. stagnalis* [30, 31]. Notably, the activation of exactly peptidergic neurons in response to increased glucose concentration in hemolymph is perhaps a common reaction for many mollusk species. At the same time, these cells may release both insulin, e.g., in *Aplysia californica* [32], and other regulatory peptides, e.g., gastrin/cholecystokinin-like in *Helix lucorum* [33].

Changes in temporal characteristics of the falling and undershoot spike phases under hyperglycemia must be associated with a modification of membrane K^+ conductance. The prolongation of these phases indicates a partial blockade of K^+ currents across the membrane rather than their activation, as is typical for mammalian brainstem neurons [34] and neurosecretory cells in the crab *Cancer borealis* [24]. Meanwhile, a whole group of vertebrate [35] and invertebrate [36] potassium channels, the so-called ATP-sensitive K^+ (K_{ATP}) channels, turn into a closed state with an increase in the interstitial glucose content, thus reducing K^+ conductance and providing membrane depolarization, as was exactly observed in our work (see Fig. 2a). However, the structure of these channels lacks a voltage sensor, and therefore, their involvement in the spike development appears unlikely. At the same time, there is evidence of ATP-sensitivity of true, voltage-gated potassium channels in the neuronal membrane [37], manifested in the inhibition of potassium currents, which may underlie the effects we observed here.

The possible osmotic effects associated with prolonged exposure of a hyperglycemic bath solution to CNS preparations deserve to be dwelt upon individually. The calculated osmotic concentration of the Ringer's solution for *L. stagnalis* was about 130 mosmol/L. As a consequence, an increase in its glucose content up to 10 mM leads to an increase in the osmolarity of such a solution by only 7–8%. Although it is well known that an increase in the hemolymph osmotic force leads to the limitation of synthesis and accumulation of peptide hormones, i.e. regulates the activity of neurosecretory dark green cells in *L. stagnalis* central nerve ganglia [38], these changes in osmolarity must be significantly higher, 160–190 mosmol/L. Moreover, the increased glucose content in

L. stagnalis hemolymph (up to 5 mM) elicits no statistically significant fluctuations in its osmotic concentration [39], which collectively confirms the idea of the impact of glucose itself rather its osmotic effects.

Thus, the unification of responses of neurosecretory cell, observed in the *L. stagnalis* CNS under hyperglycemic conditions, represents a kind of "compensation" for the desynchronization of electrical activity due to reduction in the VD1/RPaD2 coupling ratio (electrical decoupling). Viewed from this perspective, glucose can be considered as a factor which provides under hyperglycemic conditions the establishment of a new pattern of electrical activity in at least the groups of *L. stagnalis* brain peptidergic neurons and, hence, a certain behavioral pattern (similar relationships between different forms of mollusk behavior can be observed, e.g., under the effect of a temperature factor [40]). It has also been reported [41] that the electrical activity of the central dopaminergic interneurons in the *L. stagnalis* food network determines the formation of phenotypes characteristic of hungry (satiated) individuals, i.e., when the differences in hemolymph glucose content are most noticeable [14], while the locomotor serotonergic PeA-cluster motoneurons in the *L. stagnalis* pedal ganglia respond to glucose application by changes in the membrane potential and firing rate [42]. Whether the reactions described in this work are universal and applicable to interneurons of other chemical identity (e.g., containing such low-molecular-weight neurotransmitters as dopamine, serotonin, etc.) and not referring to neurosecretory (neurohormonal) cells requires additional experimental testing.

AUTHORS' CONTRIBUTION

Conceptualization and experimental design (A.V.S.); data collection (A.V.S., V.N.Sh.—electrophysiology); data treatment (A.V.S., V.N.Sh.); writing and editing the manuscript (A.V.S., V.N.Sh.).

FUNDING

This work was supported by the Belarusian Republican Foundation for Fundamental Research (grant B22-105).

COMPLIANCE WITH ETHICAL STANDARDS

All applicable international, national and/or institutional guidelines for the care and use of animals have been followed. This article does not contain the results of any research involving humans as research subjects.

CONFLICT OF INTEREST

The authors declare that they have no conflict of interest.

REFERENCES

1. Getting PA (1989) Emerging principles governing the operation of neural networks. Ann Rev Neurosci 12: 185–204. https://doi.org/10.1146/annurev.ne.12.030189.001153
2. Marder E, Calabrese RL (1996) Principles of rhythmic motor pattern generation. Physiol Rev 76: 687–717. https://doi.org/10.1152/physrev.1996.76.3.687
3. Skinner FK, Kopell N, Marder E (1994) Mechanisms for oscillation and frequency control in reciprocal inhibitory model neural networks. J Comput Neurosci 1: 69–87. https://doi.org/10.1007/BF00962719
4. Grillner S (2006) Biological pattern generation: the cellular and computational logic of networks in motion. Neuron 52: 751–766. https://doi.org/10.1016/j.neuron.2006.11.008
5. Berry MS, Pentreath VW (1977) The integrative properties of electrotonic synapses. Comp Biochem Physiol A 57: 289–295. https://doi.org/10.1016/0300-9629(77)90193-1
6. Dickinson PS, Mecsas C, Marder E (1990) Neuropeptide fusion of two motor pattern generator circuits. Nature 344: 155–158. https://doi.org/10.1038/344155a0
7. Tups A, Benzler J, Sergi D, Ladyman SR, Williams LM (2017) Central regulation of glucose homeostasis. Comp Physiol C 7: 741–764. https://doi.org/10.1002/cphy.c160015.
8. Steinbusch L, Labouèbe G, Thorens B (2015) Brain glucose sensing in homeostatic and hedonic regulation. Trends Endocrinol Metab 26: 455–466.

https://doi.org/10.1016/j.tem.2015.06.005
9. Bean BF (2007) The action potential in mammalian neurons. Nature Reviews, Neuroscience 8: 451–461. https://doi.org/10.1038/nm2148
10. Kennedy MB (2016) Synaptic signaling in learning and memory. Cold Spring Harbor Perspect Biol 8: a016824. https://doi.org/10.1101/cshperspect.a016824
11. Kerkhoven RM, Croll RP, Van Minnen J, Bogerd J, Ramkema MD, Lodder H, Boer HH (1991) Axonal mapping of the giant peptidergic neurons VD1 and RPD2 located in the CNS of the pond snail *Lymnaea stagnalis*, with particular reference to the innervation of the auricle of the heart. Brain Research 565: 8–16. https://doi.org/10.1016/0006-8993(91)91730-O.
12. Bogerd J, Geraerts WP, Van Heerikhuizen H, Kerkhoven RM, Joosse J (1991) Characterization and evolutionary aspects of a transcript encoding a neuropeptide precursor of Lymnaea neurons, VD1 and RPD2. Brain Res Mol Brain Res 11: 47–54. https://doi.org/10.1016/0169-328x(91)90020-x
13. Sidorov AV, Shadenko VN (2021) Electrical activity of identified neurons in the central nervous system of a mollusk *Lymnaea stagnalis* under acute hyperglycemia. J Evol Biochem Physiol 56: 1257–1266. https://doi.org/10.1134/S0022093021060065
14. Scheerboom JEM, Hemminga MA, Doderer A. (1978) The effects of a change of diet on consumption and assimilation and on the haemolymph-glucose concentration of the pond snail *Lymnaea stagnalis* (L). Proc Kon Ned Akad Wet, Ser C 81: 335–346.
15. Benjamin PR, Winlow W (1981) The distribution of three wide-acting synaptic inputs to identified neurones in the isolated brain of *Lymnaea stagnalis* (L.). Comp Biochem Physiol 70A:293–307. https://doi.org/10.1016/0300-9629(81)90182-1
16. Soltanov VV, Burko VE (2005) Computer programs for electrophysiological data-processing. News of Biomed Sci 1: 91–95. (In Russ).
17. Benjamin PR, Pilkington JB (1986) The electrotonic location of low-resistance intercellular junctions between a pair of giant neurones in the snail Lymnaea. J Physiol 370: 111–126. https://doi.org/10.1113/jphysiol.1986.sp015925
18. Mersman BA, Jolly SN, Lin Z and Xu F (2020) Gap Junction Coding Innexin in Lymnaea stagnalis: Sequence Analysis and Characterization in Tissues and the Central Nervous System. Front. Synaptic Neurosci 12: 1. https://doi.org/10.3389/fnsyn.2020.00001
19. Scemes E, Spray DC, Meda P (2009) Connexins, pannexins, innexins: novel roles of "hemi-channels". Pflügers Arch—Eur J Physiol 457: 1207–1226. https://doi.org/10.1007/s00424-008-0591-5
20. Gorman ALF, Mirolli M. (1972). The passive electrical properties of the membrane of a molluscan neurone. J Physiol 227: 35–49. https://doi.org/10.1113/jphysiol.1972.sp010018
21. Qazzaz MM, Winlow W (2017) Modulation of the Passive Membrane Properties of a Pair of Strongly Electrically Coupled Neurons by Anaesthetics. EC Neurology 6(4): 187–200.
22. Copping J, Syed NI, Winlow W (2000) Seasonal plasticity of synaptic connections between identified neurones in Lymnaea. Acta Biol Hung 51: 205–210.
23. Calabresi P, Marfia GA, Centonze D, Pisani A, Bernardi G (1999) Sodium influx plays a major role in the membrane depolarization induced by oxygen and glucose deprivation in rat striatal spiny neurons. Stroke 30: 171–179. https://doi.org/10.1161/01.str.30.1.171
24. Glowik RM, Golowasch J, Keller R, Marder E (1997) D-glucose-sensitive neurosecretory cells of the crab *Cancer borealis* and negative feedback regulation of blood glucose level. J Exp Biol 200: 1421–1431. https://doi.org/10.1242/jeb.200.10.1421
25. Kandel ER (1976) Cellular basis of behavior: an introduction to behavioral neurobiology. WH Freeman, San Francisco. 727 p.
26. Bukauskas FF, Verselis VK (2004) Gap junction channel gating. Biochim Biophys Acta 1662: 42–60. https://doi.org/10.1016/j.bbamem.2004.01.008
27. Sidorov AV (2012) Effect of hydrogen peroxide on electrical coupling between identified Lymnaea neurons. Invert Neurosci 12: 63–68. https://doi.org/10.1007/s10158-012-0128-7
28. Bennett MV, Contreras JE, Bukauskas FF, Saez JC (2003) New roles for astrocytes: gap junction hemichannels have something to communicate. Trends Neurosci 26: 610–617. https://doi.org/10.1016/j.tins.2003.09.008
29. Spray DC (1998) Gap junction proteins: where they live and how they die. Circ Res 83: 679–681. https://doi.org/10.1161/01.res.83.6.679
30. Kits KS, Bobeldijk RC, Crest M, Lodder JC (1991) Glucose-induced excitation in molluscan central neurons producing insulin-related peptides. Pflügers Arch 417: 597–604. https://doi.org/10.1007/BF00372957
31. Sidorov AV, Shadenko VN (2022) Electrical

properties of the sensory neuron and defense reactions of mollusc *Lymnaea stagnalis* at conditions of prolonged hyperglycemia. Experimental Biology and Biotechnology 1: 23–38. (In Russ). https://doi.org/10.33581/2957-5060-2022-1-23-38

32. Floyd PD, Li L, Rubakhin SS, Sweedler JV, Horn CC, Kupfermann I, Alexeeva VY, Ellis TA, Dembrow NC, Weiss KR, Vilim FS (1999) Insulin prohormone processing, distribution, and relation to metabolism in *Aplysia californica*. J Neurosci 19: 7732–7741. https://doi.org/10.1523/JNEUROSCI.19-18-07732.1999
33. Shevelkin AV (1994) Facilitation of defense reactions during the consumption of food in snails: the participation of glucose and gastrin/cholecystokinin-like peptide. Neurosci Behav Physiol 24: 115–124. https://doi.org/10.1007/BF02355661
34. Burdakov D, Lesage F (2010) Glucose-induced inhibition: how many ionic mechanisms? Acta Physiol (Oxf) 198: 295–301. https://doi.org/10.1111/j.1748-1716.2009.02005.x
35. Huang CW, Huang CC, Cheng JT, Tsai JJ, Wu SN (2007) Glucose and hippocampal neuronal excitability: role of ATP-sensitive potassium channels. J Neurosci Res 85: 1468–1477. https://doi.org/10.1002/jnr.21284
36. Inoue I, Tsutsui I, Brown ER (1997) K^+ accumulation and K^+ conductance inactivation during action potential trains in giant axons of the squid Sepioteuthis. J Physiol 500: 355–366. https://doi.org/10.1113/jphysiol.1997.sp022026
37. Ye R, Liu J, Jia Z, Wang H, Wang Y, Sun W, Wu X, Zhao Z, Niu B, Li X, Dai G, Li J (2016) Adenosine triphosphate (ATP) inhibits voltage-sensitive potassium currents in isolated Hensen's cells and nifedipine protects against noise-induced hearing loss in guinea pigs. Med Sci Monit 22: 2006–2012. https://doi.org/10.12659/msm.898150
38. Roubos EW, Moorer-Van Delft CM (1976) Morphometric in vitro analysis of the control of the activity of the neurosecretory dark green cells in the freshwater snail *Lymnaea stagnalis* (L.). Cell Tissue Res 174: 221–231. https://doi.org/10.1007/BF00222160
39. Sidorov AV (2022) Hemolymph osmolality in mollusk *Lymnaea stagnalis* during acute experimental hyperglycemia. Experimental Biology and Biotechnology 1: 85–89. (In Russ). https://doi.org/10.33581/2957-5060-2022-3-85-89
40. Sidorov AV (2003) Effects of temperature on respiration, defensive behavior and locomotion of fresh-water snail *Lymnaea stagnalis*. Zhurnal vysshei nervnoi deyatel'nosti im IP Pavlova 53: 513–517. (In Russ).
41. Crossley M, Staras K, Kemenes G (2018) A central control circuit for encoding perceived food value. Sci Adv 4: eaau9180. https://doi.org/10.1126/sciadv.aau9180
42. Dyakonova V, Hernádi L, Ito E, Dyakonova T, Zakharov I, Sakharov D (2015) The activity of isolated snail neurons controlling locomotion is affected by glucose. Biophysics (Nagoya-shi) 11: 55–60. https://doi.org/10.2142/biophysics.11.55

Translated by A. Polyanovsky